COMPUTER-AIDED CIVIL AND INFRASTRUCTURE ENGINEERING

Computer-Aided Civil and Infrastructure Engineering **31** (2016) 813–825

Acceleration-Based Automated Vehicle Classification on Mobile Bridges

Chul Min Yeum, Shirley J. Dyke* & Ricardo E. Basora Rovira

Lyles School of Civil Engineering, Purdue University, West Lafayette, IN 47907, USA

Christian Silva

School of Mechanical Engineering, Purdue University, West Lafayette, IN 47907, USA

&

Jeff Demo

Luna Innovation Inc., Roanoke, VA 24011, USA

Abstract: *Mobile bridges have been used for a broad range of applications including military transportation or disaster restoration. Because mobile bridges are rapidly deployed under a wide variety of conditions, often remaining in place for just minutes to hours, and have irregular usage patterns, a detailed record of usage history is important for ensuring structural safety. To facilitate usage data collection in mobile bridges, a new acceleration-based vehicle classification technique is proposed to automatically identify the class of each vehicle. Herein we present a new technique that is based on the premise that each class of vehicles produces distinctive dynamic patterns while crossing this mobile bridge, and those patterns can be extracted from the system's acceleration responses. Measured acceleration signals are converted to time–frequency images to extract two-dimensional patterns. The Viola–Jones object detection algorithm is applied here to extract and classify those patterns. The effectiveness of the technique is investigated and demonstrated using laboratory and full-scale mobile bridges by simulating realistic scenarios.*

1 INTRODUCTION

Mobile bridges are an essential structure to facilitate short-term mobility when faced with natural or man-made obstacles. Mobile bridges are often deployed for use over a period of just minutes or may on occasion remain on site for days or weeks (Basora, 2015). When such a bridge is deployed, it is necessary to rapidly confirm that it is safe to cross before use or entry. Typically, such evaluation is based on a combination of onsite physical evaluation and usage history, and thus a simple, computationally efficient, and automated approach to record actual usage is needed. To provide such a record, it would be best to determine the class of each vehicle that crosses the bridge as actual usage is monitored. Historically, a passive sensor known as a remaining service life indicator (RSLI) has been used (Department of the Army, 2006). It consists of four metallic "filaments" that are designed to fracture progressively as the bridge is subjected to loading corresponding to a specific number of cycles due to vehicle crossings. However, this approach yields a conservative and imprecise evaluation of a bridge's condition because the sensor is designed to only indicate when the bridge has been subjected to a specific number of vehicle crossings under a fixed installation and load setup. This approach was not developed with the intension to provide the granularity needed to count the number of each class of vehicles that cross the mobile bridge while emplaced in a given location. To address this need, we developed an approach to monitor actual usage of such a mobile bridge. The algorithm has the capability to identify and record the class

*To whom correspondence should be addressed. E-mail: *sdyke@purdue.edu*.

DOI: 10.1111/mice.12212

of each vehicle traversing a given mobile bridge. Acceleration measurements can be readily implemented on such a bridge, and are the basis of the approach.

The estimation of vehicle types or axle loads is an important consideration in the rating and safety of permanent bridges and roads. Several successful, commercially available systems exist for measuring a vehicle's gross and axle weights (Cardinal, 2015; TDC System, 2015) in roadways and permanent bridges. Weigh-in-motion (WIM) systems have been developed to estimate axle loads although vehicles are moving at standard speeds. However, despite many efforts to explore noninvasive approaches, it seems that the surface must inevitably be modified for sensor installation to place sensors close to the surface for direct force or strain measurement. To overcome this need, a bridge WIM system (B-WIM) has been developed (Wall et al., 2009; Cestel, 2015). B-WIM can estimate axle spacing and weight by using an influence line of the bridge, which is used to initially calibrate the system using known loads or vehicles. B-WIM is known to produce similar results as traditional WIM, while avoiding the requirements imposed by direct measurements.

Another approach relies on acceleration-based vehicle classification (Bhachu et al., 2011; Ma et al., 2014). Commercial automatic vehicle classification systems (AVC) use both accelerometers and magnetometers to detect vehicle presence and movement using estimated axle spacing (Ma et al., 2014). Axle spacing is computed using vehicle speed and axle detection based on magnetometers and accelerometers, respectively. As with strain-based WIM systems, sensors are embedded in the road surface. Displacement estimation from the measured acceleration is used for this application by using a proportional relationship between bridge deflection and vehicle weights. Researchers have also developed algorithms to estimate bridge displacement by reducing integration noise and using low-frequency accelerometers (Gindy et al., 2008; Kandula et al., 2012). For such processes, accelerometers must have low high-frequency noise and must also be frequently calibrated to remove drift errors. Multisensor data fusion methods have also been proposed to minimize such requirements and to achieve accurate estimation (Park et al., 2013; Kim et al., 2014). Although these methods are quite effective in permanent bridges, the temporary bridge is set up under a wide variety of, usually unknown, boundary conditions.

Lastly, vision (camera)-based vehicle classification is widely used for traffic surveillance and flow estimation (Rabie et al., 2005; Wei et al., 2013, 2015). However, although this approach has been successful in other situations, mobile bridges are often placed at remote sites for short periods of time and with very low power available, the use of camera would be impractical in those locations for vehicle classification.

These approaches are quite effective for their intended applications. However, there are several reasons that they are not suitable for mobile bridges. First, any modification of the bridge itself for sensor installation is prohibited. Limited space is allocated for placing sensors, and even a small intrusion to bridge surfaces would compromise the integrity of the bridge itself. Second, due to the broad range of operating conditions under which the bridge is used (boundary conditions, lengths, and elevations in each emplacement) as well as practical aspects associated with rapid implementation in the field, manual *in situ* calibration is not possible. Third, the typical sensors used in such systems are not suitable for long-term use in extremely harsh environmental conditions. For example, conventional strain gauges are subject to challenges regarding adhesion of the sensors and compensation for temperature (Espion and Halleux, 2000).

The characteristics of mobile bridges do lend themselves well to the vehicle classification problem. First, the dimensions and properties of each physical bridge of a given model that are manufactured are quite standardized. Thus, the dimensions and materials of the bridge itself can be assumed to be consistent from bridge to bridge. Second, vehicles are classified into several discrete load classes, and the classification system to be used may be defined in advance. For instance, one option is to adopt the military load classification (MLC) system up to 40 MLC, which is a standard vehicle classification system used by the Army based on hypothetical vehicles. Any vehicle around the world can be classified according to its MLC value (Department of the Army, 2008). Third, although the vehicles can traverse the bridge in either direction, the actual speed variation of vehicles is relatively small. The speed limit on such bridges is low (under 40 km/h), and stopping or accelerating are not permitted during driving (Department of the Army, 2006). This restriction indicates that similar and consistent speed patterns will be observed for all vehicles and the bridge owner has the ability to choose additional restrictions (Basora, 2015). Finally, the significant dynamic vehicle–structure interactions due to the similar mass of the vehicle and the bridge suggest that there will be distinct characteristics in the acceleration patterns that can be extracted and exploited for vehicle classification. The coupled vehicle-bridge system is a linear, time-varying dynamic system (Pesterev and Bergman, 1997; Giraldo, 2002; Xu et al., 2010; Zhang and Xia, 2013). These specific advantages highlight the potential for implementation of pattern recognition-based vehicle classification approach for mobile bridges.

Herein we develop and demonstrate a novel technique to classify vehicles and record usage patterns based on acceleration measurements. First, acceleration signals recorded when each vehicle traverses the bridge are converted into time–frequency images as spectrograms (Zhou and Adeli, 2003). Then, distinguishable patterns contained within those images are automatically extracted for classification. An image-based object classification algorithm is implemented to extract those intrinsic patterns and train robust classifiers based on predesigned discrete vehicle classes. Training of the classifiers is performed in advance using a variety of vehicles and bridge setup conditions. Once classifiers are constructed for each vehicle class on a particular bridge model, the system must simply apply those to the acceleration measurements when a vehicle crosses the bridge. There is no need for manual *in situ* calibration or additional sensor measurements.

Experimental validation of this novel automated vehicle classification method for mobile bridges is performed in two experiments. In each experiment, we categorize the available vehicles into discrete classes according to vehicle type. Experiments are conducted to realistically investigate the capabilities of the approach, and to demonstrate its potential for use on a mobile bridge. We systematically examine the capabilities of the technique under a range of conditions that will be experienced by mobile bridges, and achieve high success rates.

When dealing with mobile bridges, the approach has several advantages over existing vehicle classification techniques. First, it provides an accurate number of crossing as well as classes of vehicles, which are useful and informative for evaluation of a bridge's condition. RSLI only approximated the number of cycles of fixed load. Second, it enables fully automated vehicle classification without manual calibration, and uses inexpensive acceleration sensors that are easy to install and maintain without modification to the bridge. Furthermore, the approach is intended for field applications, and relies on the fact that training can be performed in advance with a variety of vehicles, speeds, and bridge setups (boundary conditions and bridge lengths) based on the requirements of the bridge owner. Thus, classifiers trained in advance can be applied to every bridge of that design/model.

2 VEHICLE CLASSIFICATION APPROACH

The fundamental idea behind the proposed technique is that each class of vehicles crossing a mobile bridge produces distinguishable dynamic (acceleration) patterns. Contrary to the case of permanent bridges, significant dynamic coupling between a mobile bridge and each class of vehicles are expected and their patterns are distinct and observable for classification. The dominant features of these patterns are preserved even with reasonable variations in the vehicle's speed or mass. Such dynamic patterns appear in both temporal and spectral domains, so features from both domains must be considered for robust classification.

Conceptually, this problem is analogous to visual object recognition and we adopt algorithms that have been successful for that purpose. In facial recognition, a human observer can intuitively detect the "differences" among various faces by automatically integrating several specific features as well as overall patterns even under different angles or lighting conditions. Modern object classification algorithms in the computer vision field have sought to mimic the human's "difference" detection capability and have made tremendous gains (Everingham et al., 2010). Our technique applies those powerful algorithms to tackle this vehicle classification problem for vehicles traversing a mobile bridge. The method is not intended for permanent bridge installations that are not exposed to such a wide variety of operating conditions.

There are a number of challenges to overcome for real-world implementation of vehicle classification on a mobile bridge (Basora, 2015). Because in each new installation, the bridge will be emplaced in a new location with entirely new operating conditions, the *in situ* dynamics of the bridge may vary greatly. Boundary conditions, environmental conditions, and even the length of the bridge will vary, and thus the dynamic patterns produced by a particular vehicle traversing the bridge may not be consistent across this range of setups. The dynamic patterns associated with different lengths or boundary conditions will be uncorrelated or have much weaker correlation than the patterns associated with similar bridge setups. Further, it is unreasonable to collect training data for every possible boundary condition and length. However, with a large number of identical mobile bridges in the field, it would be quite reasonable to collect data from many crossings for application to the entire inventory of mobile bridges. To address this challenge, our implementation of the technique first calls for the identification of the closest bridge setup by driving a known vehicle, called a reference vehicle, across the bridge just after bridge emplacement. Because the collection of training data already includes data obtained with the reference vehicle, we first identify the closest classifier that matches the data obtained from a new bridge setup. This classifier is used for subsequent vehicle crossings. This approach is demonstrated in the experiment discussed in Section 3. The reference vehicle can be, for example,

Fig. 1. Overview of the acceleration-based vehicle classification method for mobile bridges.

the truck responsible for transporting the bridge, although any vehicle can be used for this purpose.

The vehicle classification procedure, including training and testing phases, is shown in Figure 1. In the training stage, a variety of bridge setups are replicated by altering the bridge length, boundary materials or boundary elevation to collect data for the range of setups under which the bridge is expected to be deployed. In each bridge setup (or configuration), acceleration data would be collected across the general MLC classes of vehicles including the selected reference vehicle. However, the bridge owner may freely assign the classes for the vehicle types, and use of the MLC classes is not required. A bridge setup classifier, denoted by BSC in the figure, is trained using only data associated with a reference vehicle. Vehicle classifiers are also trained using data collected from each class of vehicle under the corresponding bridge setup, denoted by VCB in the figure. Note that a single vehicle class may contain several vehicles and models. This process is implemented one time, and then the resulting classifiers are applicable to all bridges of that model that are manufactured. At the time of deployment, a reference vehicle first traverses the bridge and acceleration responses are collected. The method will automatically apply the bridge setup classifier to those data to identify the bridge setup that is closest to the current one. Once that similar bridge setup is detected, the corresponding vehicle classifier is simply applied when new data are acquired from vehicles needing classification.

Some assumptions are made, which are quite reasonable for such a mobile/temporary bridge: (1) one vehicle is crossing the mobile bridge at a time, (2) a given bridge setup does not vary greatly during usage, (3) vehicles traverse the bridge with a reasonably constant speed, and (4) vehicles within a given class of vehicles all produce similar dynamic patterns. The foundation for assumption (4) is that the similar axle load and the number of wheels and wheelbases, which are used for constructing the standardized MLC index, are the dominant factors in producing the dynamic patterns on a mobile bridge. The steps required to implement the method are discussed subsequently.

2.1 Data acquisition

Step 1 is to acquire vertical acceleration signals from sensor nodes when the vehicle is traversing the mobile bridge. All sensors are triggered simultaneously when a vehicle enters the bridge. There are a number of techniques available to detect true event signals and differentiate them from noise, such as a short-term average/long-term average (STA/LTA) ratio method or threshold triggering (Jakka and Siddharth, 2015). The basic idea behind such methods is to capture sudden amplitude changes (increase/decrease) or fluctuations. These large changes/fluctuations do not typically occur in noise. In general, a vehicle entry event produces large accelerations similar to an impact load and the change can easily be distinguished. Thus, such methods are effective and applicable for our purpose.

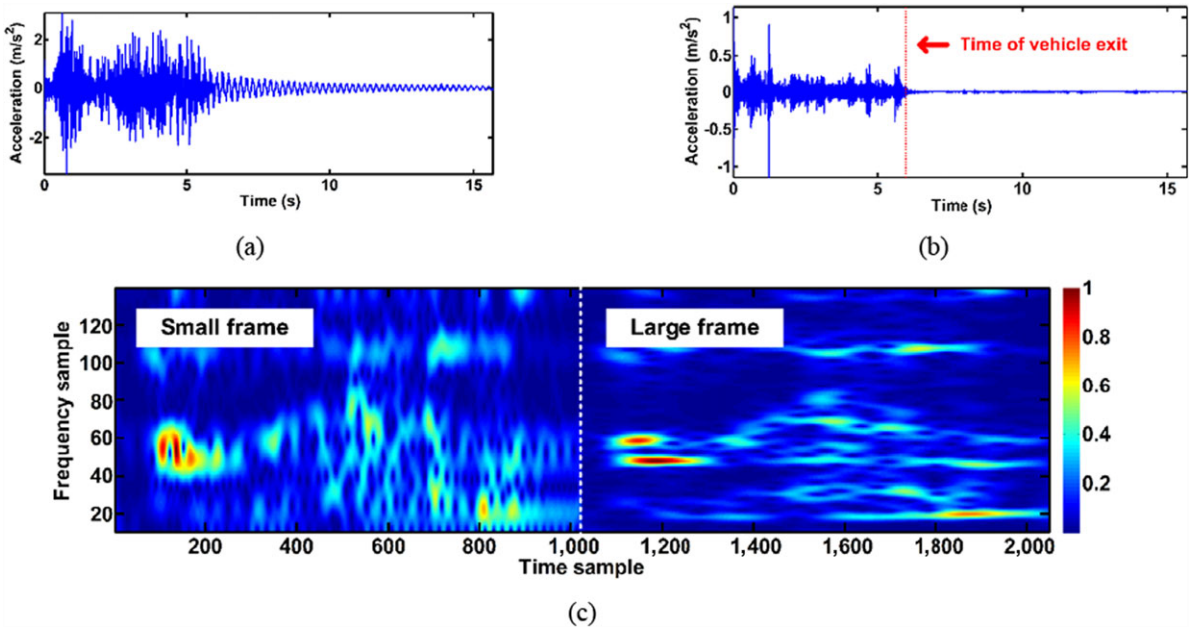

Fig. 2. Transformation of an acceleration signal to an image: (a) raw signal in *step 1*, (b) applying a high-pass filter for estimating vehicle exit time in *step 2*, and (c) spectrogram image in *step 3*.

Step 2 is to estimate the time at which the vehicle exits the bridge. The acceleration record to be used for classification should only contain data acquired although the vehicle is traversing the bridge. In general, the triggering algorithms used in *step 1* can be applied in reverse to stop (exit triggering) recording data in the sensors. However, if the sudden exit of a vehicle acts as a large impact (releasing) force on the bridge and produces transient vibration, it would be difficult to estimate the time a vehicle exits using a simple amplitude-based threshold triggering method. Figure 2a presents a typical signal acquired in *step 1* collected from the lab-scale experiment in Section 3. Unlike the sudden jump at the entrance of the vehicle, the response gently decreases at the exit.

To address this issue, we use the fact that the transient vibration is determined by the bridge's dynamic characteristics, which are mainly composed of low frequencies. A high-pass filter is implemented to filter out the transient vibration of the bridge and retain the high-frequency components induced by vehicle crossing and noise. A conservative value of the cutoff frequency of the high-frequency filter is estimated based on the modal characteristic of the bridge, and roughly set to a value higher than the third natural frequency to capture the dominant dynamics. This process enhances the transition from a valid signal (the vehicle is on the bridge) to noise (the vehicle has exited the bridge) by reducing the free vibration of the bridge due to an impact load resulting from a vehicle exit. With this filter in place, the triggering methods used in *step 1* are applied to the filtered signals in reverse order to identify the exit time. In this study, a threshold triggering method is used here to determine the exit time, and its threshold is estimated based on the background noise floor, which is measured with ambient conditions. The noise signals are assumed to follow a Gaussian distribution with a zero mean and standard deviation of σ, and the threshold limits are set to $\pm \alpha\sigma$, where α is a scaling factor typically set to 3 or greater.

Figure 2b represents the signal in Figure 2a after a high-pass filter has been applied. The boundary between the valid signal and noise is much clearer here than in the record in Figure 2a. The red dotted line denotes the estimated exit time using this reversed threshold triggering method. Note that the filtered signal is only used for determination of the exit time and cropping the original signal.

2.2 Image transformation

Using the prior steps, valid acceleration signals, which are restricted to the time when a vehicle is crossing the bridge, are obtained by cropping the measured raw signals to start at the entrance time and end at the exit time. Here, we address how this time signal is transformed into an image to become the subject image for object classification. A spectrogram, a visual

representation of a time–frequency signal, is selected for image transformation because this enables extracting features for classification using both time and frequency information. A wavelet transform may also be used for this process. A spectrogram is a simple two-dimensional grayscale image. However, further manipulation is necessary to extract consistent and robust features for classification from these images.

The image transformation and postprocessing techniques found to be effective for this purpose can be understood within the context of general image-based object classification. First, images should be normalized with respect to their size and scales. Here, size and scale correspond to the dimension (resolution) and object scales of the images, respectively. Such normalization will preserve positional information of unique features in object appearances. For example, in facial recognition, the location of the eyes on a face should be similar pixel locations across all training and testing images. Similarly, spectrogram images transformed from acceleration time signals should be of identical size and scale to facilitate their use for vehicle classification. Thus, along the frequency axis, the number and resolution of the spectral lines (i.e., frequency increments) should be identical in all images (i.e., the same bandwidth is used). Along the time axis, the number of time steps must be identical although the time resolution may be different due to the variation in the speed of each vehicle. In this sense, if a vehicle is assumed to be moving with a constant speed, the time axis in the spectrogram images may be interpreted as the vehicle location on the bridge, rather than the actual time.

Second, the most suitable image resolution must be determined. In computer vision, general pattern and object classification do not require high-resolution images (Viola and Jones, 2001; Dalal and Triggs, 2005; Sukthankar et al., 2006; Torralba, 2009). The performance of these methods typically converges above a certain resolution. An intuitive example is that objects are still recognizable even in thumbnail images. The choice of resolution can be interpreted as the desired frequency bandwidth of the measured acceleration record because the bandwidth determines the resolution in both time and frequency. Unless the informative dynamic pattern spreads into a higher frequency range, dense time and frequency resolution are not required. Furthermore, high-frequency signals are often susceptible to noise and may not be suitable for detection of robust features. Aside from performance concerns, processing high-resolution images is also computationally expensive and time-consuming. Thus, reductions in the sampling rates and image sizes are beneficial for optimizing computational time/resources and power consumption for computation and data transmission.

The third consideration is variance normalization. For object classification, normalization of pixel values in images is a necessary step to minimize the effects of lighting variations. Normalization is interpreted as putting more weight on relative difference of pixel values rather than individual absolute ones when features are extracted. However, such a normalization process is not applicable for the purpose considered in this study. Intuitively, large and heavy vehicles produce larger amplitudes of acceleration, which may become a strong feature to use for discriminating between the classes of vehicles. Furthermore, preserving amplitude features is important to provide strong correlations between vehicles in the same class. In this study, signals are processed without variance normalization before converting them to a spectrogram image. Depending on the learning (training) algorithm, the normalization process may be required such as with the K-nearest neighbor algorithm (KNN), which computes the distance between feature vectors (Bishop, 2006). The boosting learning algorithm used in this study, introduced in the next subsection, constructs classifiers by summing weak classifiers generated from individual features and thus does not require any such normalization process (Friedman et al., 2000; Torralba et al., 2007).

Step 3 is to transform the valid acceleration signals obtained using the entrance and exit times into spectrogram images normalized in size and scale. As discussed previously, all images have the same number of points in the x (time) and y (frequency) axis, and a same spectral lines and frequency resolution. Suppose that all original signals are measured with the same sampling frequency using the sensors installed on the bridge. The sampling frequency should be determined based on the frequency band of interest. The number of time points in the spectrogram images should be set to be larger than the maximum expected number of time points to avoid aliasing when resizing (normalizing) images. This approach is used because downsampling will result in aliasing. Applying a low-pass filter in advance to prevent aliasing is not applicable in this case because a low-pass filter changes the frequency content in the signal and thus changes the spectrogram, making it difficult to compare the features in the spectrogram for classification. Note that the time resolution of the spectrogram image is also varied depending on the overlap of the fast Fourier transform (FFT) frame. In this study, the FFT frame moves forward one time point at a time, and it produces same number of time points as in the time signals.

Spectrograms are computed from original signals with the same number of points in the FFT and two different sizes of frames. The frame lengths of the short-time Fourier transform for spectrogram conversion vary by resolution in both time and frequency.

Good resolution cannot be achieved in both time and frequency with only one frame size. Thus, in this study, the spectrogram image is constructed with two spectrogram transformations using two different sizes of frames, and extracting features from appropriate time and frequency resolutions, respectively. Features used for classification will be extracted from both images, as discussed in the next subsection.

The spectrograms generated from all original signals have the same frequency values along the y axis, but are still not consistent along the time axis due to small variations in the speed. To correct this inconsistency, all spectrogram images are resized (upsampled) to have the same number of points along the x (time) axis. Figure 2c presents spectrogram images generated with the signal in Figure 2a after extracting the valid acceleration record. Each portion of the combined image has either better time or frequency resolution depending on the frame size used for spectrogram. Each portion of the image has been normalized here for visual clarity.

2.3 Training bridge setup and vehicle classifiers

Step 4 is to extract features from the processed spectrogram images obtained in the previous step. Extracted features are used for distinguishing between images generated from different vehicles. A number of feature extraction techniques have been introduced in the literature for general or specific object detection and classification (Adeli and Samant, 2000; Adeli, 2001; Adeli and Karim, 2005; O'Byrne et al., 2013; Torralba et al., 2007; Yeum and Dyke, 2015). Here, Haar-like features are implemented due to their domain-independency and computation speed (Viola and Jones, 2001). Features are computed by summing across a local rectangular region using Haar-like wavelets. For simplicity, one to four rectangular Haar-like feature windows are used, which was originally proposed by Viola and Jones (2001). However, any feature extraction technique that can represent the unique patterns contained in such images can be applied for this purpose.

Step 5 is to learn the vehicle classifiers using the extracted features. A set of robust binary classifiers for each vehicle is designed to determine whether or not the features in a test image point to the existence of a corresponding vehicle in the training data. In this study, a boosting algorithm is implemented to generate a robust classifier. Boosting is a way of combining many weak classifiers to produce a strong classifier. By updating the different weights of weak classifiers adaptively, depending on misclassification errors, the optimum strong classifier is obtained, thus minimizing misclassification errors. There are several boosting algorithms introduced in the literature, but in this study, the gentle boost algorithm, proposed by Friedman, is used because it is known as simple to implement, numerically robust, and experimentally proven for object detection (Friedman et al., 2000; Torralba et al., 2007). Similar to *step* 4, in this step, a range of feature learning (training) techniques, which can produce robust classifiers from extracted features, can be implemented for this purpose.

For multiclass classification problems, there are two general strategies: One against Rest (OvR) and One against One (OvO) (Bishop, 2006). OvR generates a single classifier per class, trained from samples of the corresponding class as positive, and all other samples as negative. On the other hand, OvO produces multiple classifiers per class, trained from samples of corresponding class as positive, and samples of all other individual classes as negative. For the K-class classification problem, OvR and OvO produce the number of K and $K(K-1)/2$ binary classifiers, respectively. In this study, we adopt OvO for our application because it heuristically provides better classification outcomes. Hereafter, these binary classifiers are called candidate classifiers, all of which are used for making a single final classification.

With multiple sensor measurements available, we can consider two approaches to classifier designs. One approach is to train measurements from all sensors together based on the assumption of strong correlation between them. The other approach is to train measurements of individual sensors installed at certain locations based on the assumption that they have stronger correlation than one using all sensor responses. If each vehicle class produces specific features at a specific sensor location, the latter approach provides better classification results. However, the amount of data available for training is reduced by one over the number of sensors, and it fails to extract general features unless there is enough data. In this study, we adopt the former, which considers all sensor data at once for training.

In addition to vehicle classifiers, bridge setup classifiers must be trained, as mentioned earlier. The bridge setup classifier detects the most similar bridge setup from the training data, which points to the data collected under conditions similar to the current one. Only data from the reference vehicle are used to construct this classifier. Features from the reference vehicle data in *step* 5 are still used, but class labels assigned in *step* 6 are for bridge setups, not vehicles.

2.4 Vehicle classification

When a mobile bridge is emplaced at a new site, the current bridge setup is first identified using the bridge setup classifier, which is trained in advance. The reference vehicle crosses over the bridge to acquire acceleration

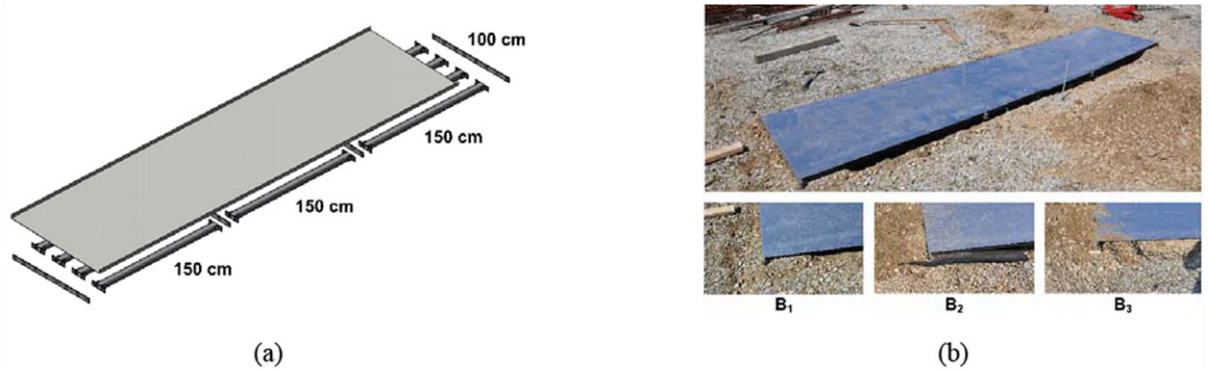

Fig. 3. Description of a lab-scale test bridge: (a) schematic of the bridge and (b) emplacement of the bridge with three different boundary conditions (bridge setups).

data from multiple sensors. Features are computed by executing *steps* 1–6. Then, the bridge setup classifier is applied to the extracted features to identify the bridge setup that is most similar to the current one and reduce the set of possible outcomes significantly. Vehicle classifiers trained with the detected bridge setup are applied to new measurements for future vehicle classification.

3 EXPERIMENTAL VALIDATION ON A LAB-SCALE BRIDGE

3.1 Experimental setup

To validate the technique under a variety of conditions, an experiment is conducted using a lab-scale bridge, as shown in Figure 3. This lab-scale experiment is intended to validate the following aspects of the technique: (1) distinguishable dynamic patterns (features) are generated and are contained within the acceleration signals; (2) the proposed technique can successfully classify vehicles into their respective classes by extracting such patterns; (3) reasonable variations in vehicle speed or the crossing direction do not affect the classification outcomes; and (4) the proposed technique is successful even when the bridge setup seen in the field is not specifically considered in the training stage.

This lab-scale bridge is dynamically similar to the full-scale rapidly emplaced bridge. Both bridges respond dynamically as a beam, with several participating modes. The vehicles are selected to have similar mass ratios and relative dynamics to the full-scale system. Thus, the dynamic interactions between the vehicles and bridges are similar to those in the full-scale bridge. It is designed to be portable, easy to mount and dismount, and can be installed using various boundary conditions and span distances. The bridge in Figure 3a is constructed using four hollow squared section beams oriented lengthwise, each constructed as three 150-cm-long segments interconnected through connection plates. The 450 cm × 100 cm bridge surface is a thin aluminum sheet with 0.1 cm thickness, and covering the entire area spanned by the beams. The bridge is emplaced across a pit in the soil with enough clearance under the bridge to eliminate any chance of contact with the ground.

To demonstrate and evaluate the performance of the classification technique, three different bridge setups are used, including: gravel (baseline ground surface condition in this location), rubber pads, and wooden supports, denoted herein as B_1, B_2, and B_3, respectively, as shown in Figure 3b. A slight ramp at each end of the bridge is created using extra soil to provide a relatively smooth entrance and exit. Data from each of the three bridge setups are collected by varying boundary support materials, although all tests use the same bridge length and elevation.

A total of eight accelerometers (PCB model 333B40), four placed along each side of the bridge, are installed to measure high-quality vertical vibration responses (PCB Piezotronics, 2015). The sensitivity, measurement range, and frequency ranges of the accelerometer are 51.0 mV/(m/s^2), 98 m/s^2 pk, and 0.5~3,000 Hz, respectively. An m+p VibPilot data acquisition system is used with 24-bit A/D converters, simultaneous sample and hold, and built-in antialiasing filters linked to the sampling rate (m+p International, 2015). A sampling frequency of 1,024 Hz is employed to acquire high-frequency signals, and also to enable an investigation of the impacts of signal processing. After data acquisition, a low-pass Butterworth filter with a 60 Hz cutoff frequency is applied to the original acceleration records, before the data are downsampled to 120 Hz. These processed signals are meant to represent measurements from typical low-cost sensors that would be used in a real implementation as well as to reduce the number of time points in the spectrogram image.

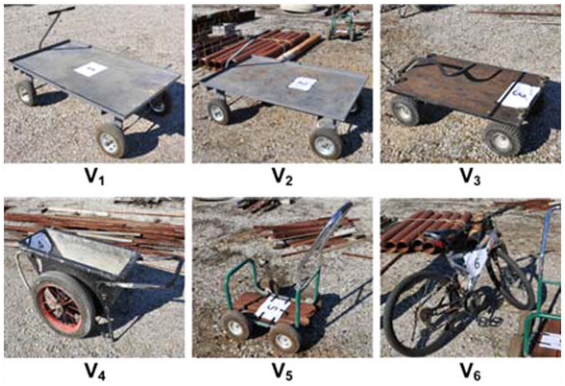

Fig. 4. Six vehicles with five different classes (note that V_1 and V_2 are same models of a vehicle).

To identify the relevant portion of the data associated with the time that the vehicle is traversing the bridge, the data acquisition is started manually before each vehicle enters the bridge. The velocity of the vehicle is not known (as it is not needed by the technique), and thus a threshold for estimating exit time based on the amplitude of the response is computed from a baseline noise signal that is then scaled by a factor of 5 (α).

Six vehicles associated with five different vehicle classes (K), denoted as V_1 to V_6, as shown in Figure 4, are driven across the bridge. V_1 and V_2 are of the same type (class) of vehicle, so data from V_2 are only used for testing, and thus are not included in the training data. The vehicle weights for V1, V3, V4, V5, and V6 are 75, 33, 70, 54, and 18 kg, and their wheelbases are 1.26, 0.79, 0 (with one axle), 0.45, and 1.17 m, respectively. Each vehicle crosses the bridge six times total, including three times from right to left and three times from left to right. All vehicles are pulled manually by three different individuals. Each vehicle begins from rest at a position outside of the bridge. Crossing duration varies (i.e., speed varies) between approximately 3 and 6 seconds depending on the vehicle class or pulling force. Two 2-wheeled vehicles (bicycles) are also included to consider different numbers of wheels and types of tires.

Hanning windows with 32 and 128 point frame sizes are used for computing the spectrograms. The numbers of FFT in each frame and time samples are consistently set to 256 and 1,024, which then define the height (y) and width (x) of the spectrogram, respectively. The resolution of spectrogram images is selected to be larger than the frame size and time points. Twenty thousand features are generated for each spectrogram image. A "strong" classifier is trained using 100 selected "weak" classifiers, which is sufficient to ensure convergence of classification (Torralba, 2009).

3.2 Vehicle classification results

Initially, the spectrogram images are examined visually to qualitatively confirm the existence of distinguishable dynamic patterns available for such classification. Figure 5 shows spectrogram images for each of the vehicles in a selected number of runs associated with B_1. Clearly, images from different runs of the same vehicle have quite similar visual patterns regarding the location and intensity of features, and images from different vehicles are often visually discernable. Also, the images from V_1 and V_2 are very similar to each other because they are the same vehicle class. This demonstrates the existence of distinguishable dynamic patterns associated with each vehicle crossing, and provides prior indication for the strong potential for interpretation of this problem within the domain of image classification.

As explained previously, it is anticipated that in a real-world implementation, the bridge emplacement would immediately be followed by a brief series of baseline crossings with a reference vehicle to identify the bridge class setup based on the existing training data, and thus increase the likelihood of successfully classifying subsequent vehicles. For this experiment, V_4 is arbitrarily assigned as the reference vehicle.

All data from V_4 are partitioned into training and testing data for cross-validation. A round is defined as when data from a single run (one record of data from a vehicle crossing) are selected for testing and the remaining are used for training. Thus, a total of 18 rounds are produced from six runs of a vehicle and three different bridge setups. For example, if a single run from B_1 is assigned for testing, the data from the other five runs using B_1 plus those from the six runs from B_2 and B_3 are used for training of each bridge setup class. A single run contains eight sensor measurements. Three candidate classifiers learned from the training data are applied to each measurement. The three candidate classifiers here are binary classifiers to differentiate between B_1 and B_2, B_1 and B_3, and B_2 and B_3, and processing produces 24 classification outcomes. Among these 24 outcomes, the outcome obtained in the majority of the classified classes is determined to be the classification if the number of occurrences exceeds a chosen threshold. If not, the outcome of the corresponding round is assigned as unclassified (UC). With the maximum number of true classification outcomes being 16 because candidate classifiers related with a specific class are two among three and they are applied to eight measurements. The threshold is thus set to 12, which is three quarters of the maximum number of true classifications. The inclusion of a UC outcome is intended to reduce the chance of false classification due to erroneous estimation of the exit time or unusual speed variations. It potentially

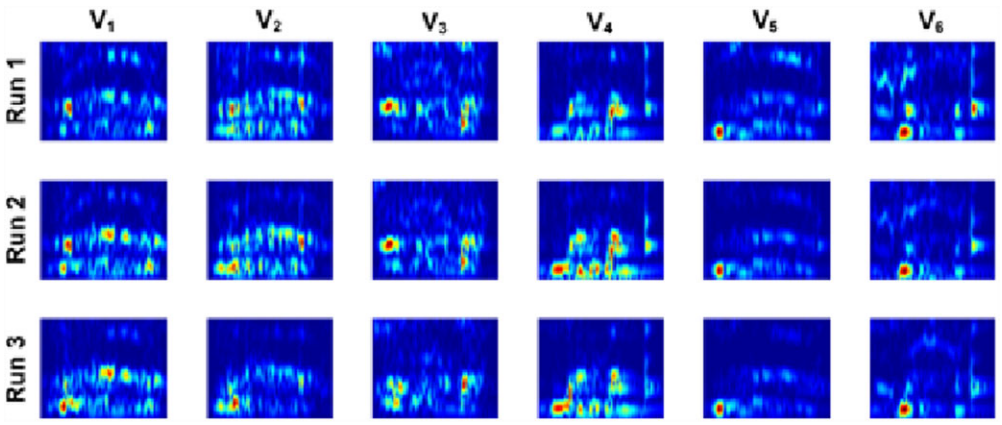

Fig. 5. Spectrogram images generated from three different crossings of six vehicles under B_1. For visual clarity, these images show only the left portion of the corresponding original spectrogram images, and are normalized.

Table 1
Confusion matrix of bridge setup classification using V_4 data

Actual \ Predicted	B_1	B_2	B_3	UC	Accuracy
B_1	6	0	0	0	100% (6/6)
B_2	0	6	0	0	100% (6/6)
B_3	0	0	6	0	100% (6/6)

would also capture situations in which vehicles are not the sources of the measured vibrations, perhaps including human, wind, or debris strikes, which do not generate the specific dynamic patterns that vehicles produce.

The classification results are provided in Table 1, in the form of a confusion matrix, commonly used to represent the performance of classification algorithms. Each entry in the matrix indicates the total number of instances each run in the actual class is classified in the corresponding predicted class. Here, in our initial classification using V_4 as the reference vehicle, we aim to classify only the V_4 data into the three classes of bridge setups. All predicted classes are correctly matched, yielding 100% classification.

Next, we validate the algorithm's ability to perform vehicle classification by classifying data records from all five classes of vehicles. Similar to the previous example, in each round, the single run data are selected for testing and the remaining are used for training. Thus, a total of 108 rounds are generated, which is the product of six runs, six vehicles, and three bridge setups. It is assumed that all bridge setups are correctly classified in advance. For instance, with the reference vehicle, in each round, vehicle classifiers are trained with data from the corresponding bridge setup and are there applied to the single remaining run. For example, if the single run data from B_1 are assigned for testing, vehicle classifiers, which are trained using the other five runs from B_1, are applied to this data for classification. In each round, 80 classification outcomes are produced and the UC threshold is set to 24, which is 75% of 32, the maximum number for true classification.

Table 2
Confusion matrix for vehicle classification (use of training and testing data collected from an identical bridge setup)

Actual \ Predicted	V_1	V_3	V_4	V_5	V_6	UC	Accuracy
V_1	18	0	0	0	0	0	100% (18/18)
V_3	0	16	0	1	0	1	88.9% (16/18)
V_4	0	0	17	1	0	0	94.4% (17/18)
V_5	0	0	0	16	0	2	88.9% (16/18)
V_6	0	0	0	1	17	0	94.4% (17/18)
V_2*	18	0	0	0	0	0	100% (18/18)

*V_2 and V_1 are the same class of vehicle.

Table 2 shows the resulting vehicle classifications. The results are quite accurate with nearly all classes being correctly classified, and only 4 of the 108 rounds being incorrectly classified. Recall that V_2 is the same vehicle model as V_1, and is not included in the training. V2 data records are only used for testing, and the true predicted class of V_2 should be V_1, as obtained in the results.

The results of this evaluation show that (1) distinguishable dynamic patterns of vehicle crossings are successfully extracted and used for classification; (2) the technique is successful even under different bridge setups; and (3) reasonable actual speed variations across all classes of vehicles do not typically affect classification results.

Next, we impose a realistic challenge by implementing the classification technique on testing data that are collected from different bridge setup included in the

Table 3
Confusion matrix for vehicle classification (training and testing data collected from different bridge setups)

Actual \ *Predicted*	V_1	V_3	V_4	V_5	V_6	UC	*Accuracy*
V_1	18	0	0	0	0	0	100% (18/18)
V_3	6	8	0	2	0	2	44.4% (8/18)
V_4	0	0	14	3	0	1	77.8% (14/18)
V_5	2	0	3	12	0	1	66.7% (12/18)
V_6	0	0	2	4	12	0	66.7% (12/18)
V_2	18	0	0	0	0	0	100% (18/18)

Fig. 6. Experimental validation using a full-scale bridge and two commercial vehicles.

training data. In reality, although a range of conditions must be used to develop a suitable set of training data, the bridge setup in the field will not be identical to one of those in the discrete set used for training. Therefore, the prior results are not entirely sufficient to fully demonstrate the effectiveness of the technique. To address this situation, we replicate these real-world challenges using our laboratory scale data. Here, data from the actual tested bridge setup are not used for training. For example, if a single run is extracted from B_1 in a round, vehicle classifiers created only from B_2 or B_3 training data are used for classification. This mimics the situation in which the current bridge setup in the field to be classified is not included in the collection of training data used to develop the classifiers.

First, the bridge setup classifier using V_4 (our reference vehicle) is applied to data from the other two bridge setups to determine which bridge setup is closest to the setup being tested, even though they may not be identical. The bridge setup classification results show that the bridge setups for B_1, B_2, and B_3 are closest to B_3, B_1, and B_1, respectively. Then, vehicle classifiers from the corresponding bridge setup are applied to data to be classified. For example, if the single run selected for testing is from B_1, vehicle classifiers trained from B_3 are used for vehicle classification.

The number of rounds in this evaluation is identical to that in the previous study. However, the bridge setup and vehicle classifiers are trained using different subsets of data. Table 3 provides the classification results, demonstrating an accurate classification of most vehicles, and less accurate results for two of the vehicles. The success in classification is always greater than 66.7% except for V_3. With different bridge setup data, the accuracy is reduced, but is much greater than a random guess, which would only yield 20% (1/K).

The relatively high accuracy obtained in these results clearly demonstrates that a given vehicle class produces similar and distinguishable dynamic patterns, even under different bridge setups. This indicates that there is great potential to apply this technique in field mobile bridge applications. With proposer understanding of the field conditions, a training data collection can be designed to replicate the common mobile bridge conditions.

4 EXPERIMENTAL VALIDATION ON A FULL-SCALE BRIDGE

To further examine the feasibility of the proposed technique, experiments are conducted using a full-scale mobile bridge. Unlike the lab-scale experiment in the previous section, evaluation with this specimen does not allow us to fully consider every aspect of the proposed technique. We are restricted to collecting data using one set of bridge setup and just two vehicles. However, this study serves to demonstrate the general application of the proposed technique using a full-scale mobile bridge. These points include the comments numbered from (1) to (3) in the first paragraph in Section 3.

A total of 12 wired accelerometers (PCB model 333B40), 6 along each edge of the bridge lengthwise, are installed to measure vertical vibrations. The data collection setup, including sampling frequency, frame size of the spectrogram, or spectrogram resolution, is identical to those used for the lab-scale experiment. Two different vehicles (sport utility vehicles), defined here as V_1 and V_2 and shown in Figure 6, are driven across the bridge in a single direction. V_1 is a 2010 Jeep Liberty Renegade, and has a wheelbase of 2.69 m and a nominal weight of 1,940 kg. V_2 is a 2003 Ford F-150 XLT, and has a wheelbase of 3.99 m and a nominal weight of 2,159 kg plus an additional 136 kg in the cargo bed. V_1 traverses the bridge five times with three unknown speeds (slow, medium, and fast). V_2 traverses the bridge four times with two unknown speeds (slow and fast). The approximate speeds described here as slow, medium, and fast are 4, 6, and 9 km/h, respectively, although these are estimated based on the total time. These variations are included to establish a broad range of data

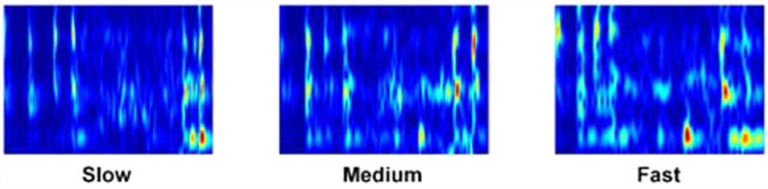

Fig. 7. Spectrogram images for V_1 from different speeds (slow, medium, and fast).

Table 4
Confusion matrix of vehicle classification for a full-scale bridge

Actual \ *Predicted*	V_1	V_2	*UC*	*Accuracy*
V_1	15	0	0	100% (15/15)
V_2	0	7	1	87.5% (7/8)

collected for training and testing. Note that the velocity of the vehicle does not need to be measured, nor is it used in the technique. A total of 23 runs are recorded.

Figure 7 shows representative spectrogram images for V_1 under reasonable speed variations (slow, medium, and fast) to qualitatively compare patterns. Clearly, the three spectrograms have similar visual patterns regarding the location, repetition, and intensity of features. Because the time needed to traverse the bridge changes with the speed, and yet the natural frequencies of the system are the same, the pattern is slightly stretched out with the normalization process. However, the method is sufficiently robust in classifying the general dynamic patterns in the spectrogram.

To evaluate the technique, 23 rounds of cross-validation are performed. In each round, a single run data record is selected for evaluation of the proposed technique and the remaining 22 records are used for training. A single-candidate classifier (i.e., $K = 2$) is applied to the 12 sensor measurements. With 12 classification outcomes, the threshold for UC is thus set to 9. The classification outcomes resulting from all 23 rounds are shown in Table 4. Near perfect classification is obtained.

5 CONCLUSION

An automated, acceleration-based vehicle classification technique is developed to specifically address the complex set of operating conditions that mobile bridge structures are subjected to in the field. The technique exploits the availability of computationally efficient image-based object classification methods, and considers a novel application of these methods to spectrograms of the vibratory responses of mobile bridges. Boosting algorithm is utilized for classifying features from spectrogram images. Both laboratory and full-scale tests are conducted to demonstrate the effectiveness of the technique by evaluating many different scenarios. In the lab-scale testing, six vehicles were classified under two different velocities and three different boundary conditions. Two of the vehicles were chosen to be in the same class. Classifiers were trained and the vehicles were classified using additional responses that were not included in the training data set. In the full-scale experiments, two vehicles were used at three different speeds, and acceleration measurements along the length of the mobile bridge were used to generate spectrograms. The results in both experiments were found to be quite successful, even under the many combinations of realistic variations in the bridge setup and vehicle speed considered in each of these cases. The technique classifies the subject vehicles with high success rates.

ACKNOWLEDGMENTS

The authors acknowledge support from Small Business Innovative Research (SBIR) Program and the Engineering Research and Development Center - Construction Engineering Research Laboratory (ERDC-CERL) under Contract No. W9132T-12-C-0020. The authors would also like to acknowledge fellowship support through the Purdue Military Research Initiative.

REFERENCES

Adeli, H. (2001), Neural networks in civil engineering: 1989–2000, *Computer-Aided Civil and Infrastructure Engineering*, **16**(2), 126–42.

Adeli, H. & Karim, A. (2005), *Wavelets in Intelligent Transportation Systems*, John Wiley & Sons, Hoboken, NJ.

Adeli, H. & Samant, A. (2000), An adaptive conjugate gradient neural network–wavelet model for traffic incident detection, *Computer-Aided Civil and Infrastructure Engineering*, **15**(4), 251–60.

Basora, R. (2015), Vehicle classification method for use with rapidly emplaced mobile bridges: a sensitivity study. Masters thesis, Purdue University.

Bhachu, K. S., Baldwin, J. D. & Mish, K. D. (2011), Method for vehicle identification and classification for bridge response monitoring, in *Dynamics of Bridges*, Volume **5**, Springer, New York, NY, pp. 93–103.

Bishop, C. M. (2006), *Pattern Recognition and Machine Learning*, Springer, New York, NY.

Cardinal (2015), Virtual weight stations. Available at: www.wimscales.com, accessed August 2015.

Cestel (2015), SiWIM measurement. Available at:www.cestel.eu, accessed August 2015.

Dalal, N. & Triggs, B. (2005), Histograms of oriented gradients for human detection, in *Proceedings of IEEE Computer Society Conference on Computer Vision and Pattern Recognition, 2005*, Vol. 1, 886–93.

Department of the Army (2006), Operator's manual for rapidly emplaced bridge (REB), TM 5-5420-280-10.

Department of the Army (2008), Field Manual 3-34.170 Engineer Reconnaissance, Appendix E.

Espion, B. & Halleux, P. (2000), Long-term measurements of strains with strain gauges and stability of strain gauge transducers, *Reports in Applied Measurement*, **3**, 1–11.

Everingham, M., Van Gool, L., Williams, C. K., Winn, J. & Zisserman, A. (2010), The Pascal visual object classes (VOC) challenge, *International Journal of Computer Vision*, **88**(2), 303–38.

Friedman, J., Hastie, T. & Tibshirani, R. (2000), Additive logistic regression: a statistical view of boosting (with discussion and a rejoinder by the authors), *The Annals of Statistics*, **28**(2), 337–407.

Gindy, M., Vaccaro, R., Nassif, H. & Velde, J. (2008), A state-space approach for deriving bridge displacement from acceleration, *Computer-Aided Civil and Infrastructure Engineering*, **23**(4), 281–90.

Giraldo, D. (2002), Control of a moving oscillator on an elastic continuum using various techniques. Masters thesis, Washington University in St. Louis.

Jakka, R. S. & Siddharth, G. (2015), Suitable triggering algorithms for detecting strong ground motions using MEMS accelerometers, *Earthquake Engineering and Engineering Vibration* **14**(1), 27–35.

Kandula, V., DeBrunner, L., DeBrunner, V. & Rambo-Roddenberry, M. (2012), Field testing of indirect displacement estimation using accelerometers, in *Proceedings of 2012 Conference Record of the 46th Asilomar Conference on Signals, Systems and Computers (ASILOMAR)*, IEEE, 1868–72.

Kim, J., Kim, K. & Sohn, H. (2014), Autonomous dynamic displacement estimation from data fusion of acceleration and intermittent displacement measurements, *Mechanical Systems and Signal Processing*, **42**(1), 194–205.

m+p International (2015), USB-Based data acquisition. Available at:www.mpihome.com, accessed August 2015.

Ma, W., Xing, D., McKee, A., Bajwa, R., Flores, C., Fuller, B. & Varaiya, P. (2014), A wireless accelerometer-based automatic vehicle classification prototype system, *IEEE Transactions on Intelligent Transportation Systems*, **15**(1), 104–11.

O'Byrne, M., Schoefs, F., Ghosh, B. & Pakrashi, V. (2013), Texture analysis based damage detection of ageing infrastructural elements, *Computer-Aided Civil and Infrastructure Engineering*, **28**(3), 162–77.

Park, J.-W., Sim, S.-H., Jung, H.-J. & Spencer, B.F.S., Jr. (2013), Development of a wireless displacement measurement system using acceleration responses, *Sensors*, **13**, 8377–92.

PCB Piezotronics (2015), ICP accelerometer (Model 333B40). Available at: www.pcb.com, accessed August 2015.

Pesterev, A. V. & Bergman, L. A. (1997), Response of elastic continuum carrying moving linear oscillator, *Journal of Engineering Mechanics*, **123**(8), 878–84.

Rabie, T., Abdulhai, B., Shalaby, A. & El-Rabbany, A. (2005), Mobile active-vision traffic surveillance system for urban networks, *Computer-Aided Civil and Infrastructure Engineering*, **20**(4), 231–41.

Sukthankar, R., Ke, Y. & Hoiem, D. (2006), Semantic learning for audio applications: a computer vision approach, in *Proceedings of Conference on Computer Vision and Pattern Recognition Workshop, 2006 (CVPRW206)*, IEEE, 112–24.

TDC system (2015), High speed weigh-in-motion and classification system. Available at: www.tdcsystems.co.uk, accessed August 2015.

Torralba, A. (2009), How many pixels make an image? *Visual Neuroscience*, **26**(1), 123–31.

Torralba, A., Kevin P. M. & William T. F. (2007), Sharing visual features for multiclass and multiview object detection, *IEEE Transactions on Pattern Analysis and Machine Intelligence*, **29**(**5**), 854–69.

Viola, P. & Jones, M. (2001), Rapid object detection using a boosted cascade of simple features, in *Proceedings of the 2001 IEEE Computer Society Conference on Computer Vision and Pattern Recognition, 2001 (CVPR 2001)*, Vol. 1, IEEE.

Wall, C. J., Christenson, R. E., McDonnell, A. M. H. & Jamalipour, A. (2009). A non-intrusive bridge weigh-in-motion system for a single span steel girder bridge using only strain measurements, No. CT-2251-3-09-5, Connecticut Department of Transportation and U.S. Department of Transportation Federal Highway Administration.

Wei, H., Abrishami, H., Xiao, X. & Karteek, A. (2015), Adaptive video-based vehicle classification technique for monitoring traffic, No. FHWA/OH-2015/20, Ohio Department of Transportation and U.S. Department of Transportation Federal Highway Administration.

Wei, H., Liu, H., Ai, Q., Li, Z., Xiong, H. & Coifman, B. (2013), Empirical innovation of computational dual-loop models for identifying vehicle classifications against varied traffic conditions, *Computer-Aided Civil and Infrastructure Engineering*, **28**(8), 621–34.

Xu, Y. L., Li, Q., Wu, D. J. & Chen, Z. W. (2010), Stress and acceleration analysis of coupled vehicle and long-span bridge systems using the mode superposition method, *Engineering Structures*, **32**(5), 1356–68.

Yeum, C. M. & Dyke, S. J. (2015), Vision-based automated crack detection for bridge inspection, *Computer-Aided Civil and Infrastructure Engineering*, **30**(10), 759–70.

Zhang, N. & Xia, H. (2013), Dynamic analysis of coupled vehicle–bridge system based on inter-system iteration method, *Computers & Structures*, **114–115**, 26–34.

Zhou, Z. & Adeli, H. (2003), Time-frequency signal analysis of earthquake records using Mexican hat wavelets, *Computer-Aided Civil and Infrastructure Engineering*, **18**(5), 379–89.